

Taxicab Correspondence Analysis of Sparse Contingency Tables

Choulakian, V., Université de Moncton, Canada,
email: vartan.choulakian@umoncton.ca;

August 2015

Abstract

Visualization and interpretation of contingency tables by correspondence analysis (CA), as developed by Benzécri, has a rich structure based on Euclidean geometry. However, it is a well established fact that, often CA is very sensitive to sparse contingency tables, where we characterize sparsity as the existence of relatively high-valued counts, rare observations discussed by Rao (1995), and zero-block structure emphasized by Novak and Bar-Hen (2005) and Greenacre (2013). In this paper, we aim to emphasize the important roles played by L_1 and L_2 geometries. This will be done by comparing the maps obtained by CA with the maps obtained by taxicab correspondence analysis (TCA), where TCA is a robust L_1 variant of correspondence analysis. If the projections of view of both maps are quite different, we refer to this phenomenon as parallax. In astronomy, parallax means the apparent change in the position of an object as seen from two different points. In our case the two different points correspond to the two different geometries, Euclidean and Taxicab. The existence of a parallax highlights the important, but hidden, role of the underlying geometry in the interpretation of the maps obtained in multivariate data analysis. We emphasize the following fact: Only by comparing CA and TCA graphical displays, we are able to reveal the phenomenon of parallax. Examples are provided.

Key words: Sparse contingency tables; correspondence analysis; taxicab correspondence analysis; rare observations; zero-block structure; parallax; influence measures; interpretable maps.

1 Introduction

Correspondence analysis (CA), developed by Benzécri (1973) since 1960s, as a statistical method for different kinds of datasets, in particular for contingency tables, is embedded both in theory and in practice. The theory is based on the chi-square distance between the profiles; parallel to this beautiful theory, the practice is entrenched in the joint interpretation of the graphical displays based on the Euclidean geometry. Seeing this extreme fondness of the use and interpretation of the maps by the users of CA, Nishisato (1998) suggested the replacement of the adage “seeing is believing“ with “graphing is believing“ and stressed the importance of interpretable graphs. Additionally, we recall the often cited quip “a picture is worth a thousand words“, and via geometric interpretation of maps CA offers much to the analysis of complex multivariate data sets. So the philosophical question asked by Schlick (2000, part 5) ”Theory and Observation: Is seeing believing ?” is quite relevant here in the context of data analysis by CA.

It is well known that, CA is very sensitive to some particularities of a data set; further, how to identify and handle these is an open unresolved problem. Here, we enumerate three under the umbrella of sparse contingency tables: First, Rao (1995) stressed the influence of rare observations (rows or columns that have relatively small marginal weights compared to others) and proposed an alternative to CA based on Hellinger distance (a square-root transformation of counts). Second, Greenacre (2013) highlighted the adverse influence of a zero-block structure in a data set and suggested its suppression from analysis. Similar to Greenacre’s observation, earlier Novak and Bar-Hen (2005) observed that a zero-block structure in a contingency table disturbs CA results, but argued against the suppression of the zero-block. Third, often few relatively high-valued cells have detrimental effect on the CA outputs by emphasizing some aspects of the data, even though apparently the interpretation of the dimensions seems meaningful to the researchers. Our approach in this paper is to highlight the above mentioned points by comparing the maps obtained by CA with the maps obtained by taxicab correspondence analysis (TCA), where TCA is a L_1 variant of CA. If the projections of view of both maps are quite different, we refer to this phenomenon as parallax. In astronomy, parallax means the apparent change in the position of an object as seen from two different points. In our case the two different points correspond to the two different geometries, Euclidean (L_2) and Taxicab (L_1). The existence of a parallax will highlight the impor-

tant, but hidden, role of the underlying geometry in the interpretation of the maps obtained in multivariate data analysis. We emphasize the following fact based on our experience: Only by comparing CA and TCA graphical displays, we are able to see the existence of the phenomenon of parallax.

This paper is organized as follows: In section 2, we introduce notation by presenting a brief comparison of CA and TCA with further comments; section 3 presents the analysis of three data sets to highlight the absence or the presence of the parallax phenomenon. And we conclude in section 4.

The theory of CA can be found, among others, in Benzécri (1973, 1992), Greenacre (1984), Gifi (1990), Le Roux and Rouanet (2004), Murtagh (2005), and Nishisato (2007); the recent book, authored by Beh and Lombardi (2014), presents a panoramic review of CA and related methods. Since 2006, Choulakian and coauthors have studied mathematical properties of TCA applied to many kinds of non-negative data; in particular, TCA of contingency tables and their comparison with CA are studied in the following papers: Choulakian (2006), Choulakian et al. (2006), Choulakian (2008), and Choulakian, Simonetti and Gia (2014).

2 Correspondence analysis and taxicab correspondence analysis: an overview

Let $\mathbf{N} = (n_{ij})$ be a contingency table cross-classifying two nominal variables with I rows and J columns, and $\mathbf{P} = \mathbf{N}/n$ be the associated correspondence matrix with elements p_{ij} , where $n = \sum_{j=1}^J \sum_{i=1}^I n_{ij}$ is the sample size. We define as usual $p_{i*} = \sum_{j=1}^J p_{ij}$, $p_{*j} = \sum_{i=1}^I p_{ij}$, the vector $\mathbf{r} = (p_{i*}) \in \mathbf{R}^I$, the vector $\mathbf{c} = (p_{*j}) \in \mathbf{R}^J$, and $\mathbf{D}_r = \text{Diag}(\mathbf{r})$ the diagonal matrix having diagonal elements p_{i*} , and similarly $\mathbf{D}_c = \text{Diag}(\mathbf{c})$. We suppose that \mathbf{D}_r and \mathbf{D}_c are positive definite metric matrices of size $I \times I$ and $J \times J$, respectively; this means that the diagonal elements of \mathbf{D}_r and \mathbf{D}_c are strictly positive. Let $k = \text{rank}(\mathbf{R}_0)$, where

$$\mathbf{R}_0 = (\mathbf{P} - \mathbf{r}\mathbf{c}')$$

is the residual matrix with respect to the independence model. CA and TCA can be considered as principal components analysis for categorical data, where \mathbf{P} or \mathbf{R}_0 is decomposed into a sum of bilinear terms shown in equation (1). Equation (1) is named the data reconstruction formula, and it is obtained by generalized singular value decomposition and its taxicab version with

respect to the metric matrices \mathbf{D}_r and \mathbf{D}_c , see in particular Choulakian, Simonetti and Gia (2014):

$$\mathbf{P} = \mathbf{D}_r(\mathbf{1}_I \mathbf{1}_J' + \sum_{\alpha=1}^k \mathbf{f}_\alpha \mathbf{g}_\alpha' / \lambda_\alpha) \mathbf{D}_c,$$

or elementwise

$$p_{ij} = p_{i*} p_{*j} \left[1 + \sum_{\alpha=1}^k f_\alpha(i) g_\alpha(j) / \lambda_\alpha \right], \quad (1)$$

where \mathbf{f}_α and \mathbf{g}_α represent the row and column factor scores, and λ_α the associated dispersion measure for $\alpha = 1, \dots, k$. Note that in both methods \mathbf{f}_α and \mathbf{g}_α are \mathbf{D}_r and \mathbf{D}_c centered respectively; that is

$$\begin{aligned} \mathbf{f}_\alpha' \mathbf{D}_r \mathbf{1}_I &= \mathbf{g}_\alpha' \mathbf{D}_c \mathbf{1}_J \\ &= 0, \end{aligned} \quad (2)$$

where $\mathbf{1}_I$ is a column vector of ones of size I .

In CA, the factor scores satisfy

$$\|\mathbf{f}_\alpha\|_{2, \mathbf{D}_r} = \mathbf{f}_\alpha' \mathbf{D}_r \mathbf{f}_\alpha / \lambda_\alpha = \|\mathbf{g}_\alpha\|_{2, \mathbf{D}_c} = \mathbf{g}_\alpha' \mathbf{D}_c \mathbf{g}_\alpha / \lambda_\alpha = \lambda_\alpha \quad \text{for } \alpha = 1, \dots, k, \quad (3)$$

$$\mathbf{f}_\alpha' \mathbf{D}_r \mathbf{f}_\beta = \mathbf{g}_\alpha' \mathbf{D}_c \mathbf{g}_\beta = 0 \quad \text{for } \alpha \neq \beta. \quad (4)$$

Equation (3) says that the \mathbf{D}_r weighted L_2 norm of \mathbf{f}_α is λ_α ; likewise, equation (4) says that \mathbf{f}_α is \mathbf{D}_r orthogonal to \mathbf{f}_β for $\alpha \neq \beta$. In CA the normed or standardized principal axes are $\mathbf{f}_\alpha / \lambda_\alpha$ for column profiles and $\mathbf{g}_\alpha / \lambda_\alpha$ for row profiles.

In TCA, the factor scores satisfy

$$\|\mathbf{f}_\alpha\|_{1, \mathbf{D}_r} = \mathbf{f}_\alpha' \mathbf{D}_r \text{sgn}(\mathbf{f})_\alpha = \|\mathbf{g}_\alpha\|_{1, \mathbf{D}_c} = \mathbf{g}_\alpha' \mathbf{D}_c \text{sgn}(\mathbf{g})_\alpha = \lambda_\alpha \quad \text{for } \alpha = 1, \dots, k, \quad (5)$$

$$\mathbf{f}_\alpha' \mathbf{D}_r \text{sgn}(\mathbf{f})_\beta = \mathbf{g}_\alpha' \mathbf{D}_c \text{sgn}(\mathbf{g})_\beta = 0 \quad \text{for } \alpha > \beta. \quad (6)$$

where $\text{sgn}(\mathbf{g}_\alpha) = (\text{sgn}(g_\alpha(1)), \dots, \text{sgn}(g_\alpha(J)))'$, and $\text{sgn}(g_\alpha(j)) = 1$ if $g_\alpha(j) > 0$, $\text{sgn}(g_\alpha(j)) = -1$ otherwise. Equation (5) says that the \mathbf{D}_r weighted L_1 norm of \mathbf{f}_α is λ_α ; likewise, equation (6) says that \mathbf{f}_α is \mathbf{D}_r orthogonal to $\text{sgn}(\mathbf{f}_\beta)$ for $\alpha > \beta$. In TCA the normed or standardized principal axes are $\text{sgn}(\mathbf{f}_\alpha)$ for column profiles and $\text{sgn}(\mathbf{g}_\alpha)$ for row profiles.

An important property of TCA and CA is that columns (or rows) with identical profiles (conditional probabilities) receive identical factor scores.

The factor scores are used in the graphical displays. Moreover, merging of identical profiles do not change the results of the data analysis; this is named the principle of equivalent partitioning by Nishisato (1984); it includes the famous distributional equivalence property, which is satisfied by CA.

2.1: Remarks

- a) CA of \mathbf{P} is equivalent to CA of \mathbf{R}_0 . Analogously, TCA of \mathbf{P} is equivalent to TCA of \mathbf{R}_0 .
- b) In CA, the principal factors \mathbf{f}_α and \mathbf{g}_α are functions of the eigenvectors of a similarity measure between the rows or columns and more importantly the similarity measure depends on the chosen metric \mathbf{D}_r and \mathbf{D}_c . We describe the computation of the principal factors \mathbf{f}_α and \mathbf{g}_α in four steps:

Step 1: we calculate the matrix of Pearson residuals,

$$\mathbf{S} = \mathbf{D}_r^{-1/2}(\mathbf{P} - \mathbf{r}\mathbf{c}')\mathbf{D}_c^{-1/2}. \quad (7)$$

Step 2: we calculate the eigenvectors \mathbf{x}_α via the eigen-equation,

$$\mathbf{S}'\mathbf{S}\mathbf{x}_\alpha = \lambda_\alpha^2\mathbf{x}_\alpha \quad \text{with} \quad \mathbf{x}_\alpha'\mathbf{x}_\alpha = 1, \quad (8)$$

where the (i, j) th element of $\mathbf{S}'\mathbf{S}$ represents a similarity measure between the two column categories i and j .

Step 3: we calculate $\mathbf{f}_\alpha = \lambda_\alpha^{-1/2}\mathbf{D}_r^{-1/2}\mathbf{x}_\alpha$.

Step 4: we calculate \mathbf{g}_α via the transition formula (22).

Rao (1995) remarked that in (7,8) rare observations have exaggerated influence in CA. Data set 2 shows that Rao's observation can sometimes be true, but not often as discussed by Greenacre (2013); additionally, Nowak and Bar-Hen (2005) developed a criterion based on the influence function to identify influential rare observations.

Compared to CA, TCA stays as close as possible to the original data: It directly acts on the correspondence matrix \mathbf{P} or \mathbf{R}_0 in the largest sense that the basic taxicab decomposition is independent of the metrics \mathbf{D}_r and \mathbf{D}_c : it is simply constructed from a sum of the signed columns or rows of the residual correspondence matrix, for further details see Choulakian

(2006); only the relative direction of the rows or columns is taken into account without calculating a similarity (or dissimilarity) measure between the rows or columns. The optimization criterion is based on the famous Grothendieck problem, see Pisier (2012). The steps for the computation of the principal factors \mathbf{f}_α and \mathbf{g}_α are done iteratively for $\alpha = 1, \dots, k$:

Step 1: we compute the principal axis

$$\mathbf{u}_\alpha = \arg \max_{\mathbf{u} \in \{-1,1\}^J} \|\mathbf{R}_{\alpha-1} \mathbf{u}\|_1,$$

where $\mathbf{R}_0 = \mathbf{P} - \mathbf{r}\mathbf{c}'$ and $\mathbf{R}_\alpha = \mathbf{P} - \mathbf{r}\mathbf{c}' - \sum_{\beta=1}^{\alpha} \mathbf{f}_\beta \mathbf{g}_\beta' / \lambda_\beta$ for $\alpha = 1, \dots, k$.

Step 2: we compute the principal factor $\mathbf{f}_\alpha = \mathbf{D}_r^{-1} \mathbf{R}_\alpha \mathbf{u}_\alpha$.

Step 3: we calculate \mathbf{g}_α via the transition formula (15).

Step 4: we update $\mathbf{R}_{\alpha+1} = \mathbf{P} - \mathbf{r}\mathbf{c}' - \sum_{\beta=1}^{\alpha+1} \mathbf{D}_r \mathbf{f}_\beta \mathbf{g}_\beta' \mathbf{D}_c / \lambda_\beta$.

- c) In TCA of \mathbf{P} both principal factors \mathbf{f}_α and \mathbf{g}_α for $\alpha = 1, \dots, k$ satisfy the equivariability property, see Choulakian (2008b). This means that \mathbf{f}_α and \mathbf{g}_α are equally balanced in the sense that

$$\begin{aligned} \frac{\lambda_\alpha}{2} &= \sum_{i \in I_{\alpha+}} p_{i*} f_\alpha(i), \\ &= - \sum_{i \in I_{\alpha-}} p_{i*} f_\alpha(i), \\ &= \sum_{j \in J_{\alpha+}} p_{*j} g_\alpha(j), \\ &= - \sum_{j \in J_{\alpha-}} p_{*j} g_\alpha(j), \end{aligned} \tag{9}$$

where $I_{\alpha+} = \{i | f_\alpha(i) > 0\}$, $I_{\alpha-} = \{i | f_\alpha(i) < 0\}$, $J_{\alpha+} = \{j | g_\alpha(j) > 0\}$ and $J_{\alpha-} = \{j | g_\alpha(j) < 0\}$. This easily follows from the fact that the principal factors \mathbf{f}_α and \mathbf{g}_α are \mathbf{D}_r and \mathbf{D}_c centered, they satisfy equation (2). An informal illustrative interpretation of the equivariability property is that TCA pulls inside potential influential observations and pushes outside points around the origin, thus providing a more balanced and robust view of data.

We note that in CA the principal factors \mathbf{f}_α and \mathbf{g}_α do not satisfy the equivariability property, because they are unequally balanced in the sense

that

$$\begin{aligned}
A &= \sum_{i \in I_{\alpha+}} p_{i*} f_{\alpha}(i), \\
&= - \sum_{i \in I_{\alpha-}} p_{i*} f_{\alpha}(i) | f_{\alpha}(i), \\
B &= \sum_{j \in J_{\alpha+}} p_{*j} g_{\alpha}(j), \\
&= - \sum_{j \in J_{\alpha-}} p_{*j} g_{\alpha}(j),
\end{aligned}$$

and in general,

$$A \neq B;$$

furthermore, A and B are not related to the dispersion measure λ_{α} , because CA maximizes the variance of the factor scores.

- d) Given that the approach in CA and TCA is geometric, influence measure of a point (a column or a row) to the α th factor is provided by the relative contribution of that point to the dispersion measure of the α th factor in per 1000 units.

In CA, based on (3), this corresponds to:

$$RC_{\alpha}(i) = 1000 \frac{p_{i*} f_{\alpha}^2(i)}{\lambda_{\alpha}^2} \quad \text{and} \quad RC_{\alpha}(j) = 1000 \frac{p_{*j} g_{\alpha}^2(j)}{\lambda_{\alpha}^2}. \quad (10)$$

In TCA, based on (5), we have the signed relative contribution

$$SRC_{\alpha}(i) = 1000 \frac{p_{i*} f_{\alpha}(i)}{\lambda_{\alpha}} \quad \text{and} \quad SRC_{\alpha}(j) = 1000 \frac{p_{*j} g_{\alpha}(j)}{\lambda_{\alpha}}. \quad (11)$$

It is important to note that, in CA,

$$0 < RC_{\alpha}(point) < 1000; \quad (12)$$

while in TCA, from (9) we get,

$$-500 \leq SRC_{\alpha}(point) \leq 500. \quad (13)$$

- e) In both methods the maps or joint displays are obtained by plotting $(\mathbf{f}_\alpha, \mathbf{f}_\beta)$ and $(\mathbf{g}_\alpha, \mathbf{g}_\beta)$ for $\alpha \neq \beta$. Both CA and TCA have common residual transition formulas, see Choulakian (2006),

$$f_\alpha(i) = p_{i*}^{-1} \sum_{j=1}^J R_{\alpha-1}(i, j) u_\alpha(j) \quad \text{for } \alpha = 1, \dots, k, \quad (14)$$

and

$$g_\alpha(j) = p_{*j}^{-1} \sum_{i=1}^I R_{\alpha-1}(i, j) v_\alpha(i) \quad \text{for } \alpha = 1, \dots, k, \quad (15)$$

where \mathbf{R}_α is the residual correspondence matrix, and \mathbf{u}_α and \mathbf{v}_α for $\alpha = 1, \dots, k$ are the normed principal axes and related to the factor scores \mathbf{g}_α and \mathbf{f}_α for $\alpha = 1, \dots, k$ in the following way. In both methods

$$\mathbf{R}_\alpha = \mathbf{P} - \mathbf{rc}' - \sum_{\beta=1}^{\alpha} \mathbf{f}_\beta \mathbf{g}_\beta' / \lambda_\beta. \quad (16)$$

In TCA

$$\mathbf{u}_\alpha = \text{sgn}(\mathbf{g}_\alpha) \quad \text{and} \quad \mathbf{v}_\alpha = \text{sgn}(\mathbf{f}_\alpha) \quad \text{for } \alpha = 1, \dots, k, \quad (17)$$

so equations (14) and (15) become

$$f_\alpha(i) = p_{i*}^{-1} \sum_{j=1}^J R_{\alpha-1}(i, j) \text{sgn}(g_\alpha(j)) \quad \text{for } \alpha = 1, \dots, k, \quad (18)$$

and

$$g_\alpha(j) = p_{*j}^{-1} \sum_{i=1}^I R_{\alpha-1}(i, j) \text{sgn}(f_\alpha(i)) \quad \text{for } \alpha = 1, \dots, k. \quad (19)$$

Equations (18) and (19) help us to interpret the joint TCA maps in the following way: $f_\alpha(i)$, the coordinate of point i on the α th axis is the signed centroid of the residual correspondence matrix within the p_{i*}^{-1} constant. Analogous interpretation applies to $g_\alpha(j)$, the coordinate of point j on the α th axis.

In CA

$$\mathbf{u}_\alpha = \mathbf{g}_\alpha / \lambda_\alpha \quad \text{and} \quad \mathbf{v}_\alpha = \mathbf{f}_\alpha / \lambda_\alpha \quad \text{for} \quad \alpha = 1, \dots, k. \quad (20)$$

The joint interpretation of column and row categories in the CA map is based on the well known transition formulas

$$f_\alpha(i) = \sum_{j=1}^J \Pr(j|i) g_\alpha(j) / \lambda_\alpha \quad \text{for} \quad \alpha = 1, \dots, k, \quad (21)$$

and

$$g_\alpha(j) = \sum_{i=1}^I \Pr(i|j) f_\alpha(i) / \lambda_\alpha \quad \text{for} \quad \alpha = 1, \dots, k, \quad (22)$$

where $\Pr(j|i) = p_{ij}/p_{i*}$, the conditional probability of observing j given i . Note that (21, 22) can be obtained from (14, 15) via (3, 4, 20). In (21), the factor score $f_\alpha(i)$ is the weighted average (centroid) of the factor scores $g_\alpha(j)$ within the λ_α^{-1} constant. Analogous interpretation applies to $g_\alpha(j)$, the coordinate of point j on the α th axis.

3 Data analysis

We analyzed many data sets, here we present a representative sample of our results. In the first data set, there is no parallax; the 2nd and 3rd data sets have different structures, and we see the phenomenon of a parallax in both. The appearance of parallax seems to be positively associated with the sparsity index of a contingency table

$$sparsity\ index = \% \text{ of zero cells.}$$

3.1: TV programs data set

Table 1 presents a contingency table of size 13×7 taken from Benzécri (1976), where a sample of 400 individuals evaluate 13 TV programs on a likert scale from 1(*excellent*) to 5(*bad*); also two other categories of response are included *noopinion* on the program and *dontknow* the program. The *sparsity index* = 0. Figure 1 displays CA and TCA maps, where we see that both maps produce the same interpretation, so there is no parallax. The % of explained variation for CA (resp. for TCA) of the first two dimensions are

70.7 (resp. 78%) and 21.6 (resp 16.7); with almost equivalent cumulative value of 92.4% for CA and 94.7 for TCA. The interpretation of the first two dimensions in Figure 1 will be based on two principles: principle of dichotomy and principle of gradation.

3.1.1: Interpretation of the 1st axis

We note that $RC_1(dontknow) = 700$ and $SRC_1(dontknow) = -500$ as given at the bottom of Table 1; so the first axis represents the dichotomy between ignorance and knowledge: where the response category *dontknow* opposes to the 5 likert response scales, *noopinion* being near the origin.

3.1.2: Interpretation of the 2nd axis

The 5 Likert response categories are ordered from *excellent* to *bad*.

3.1.3: Interpretation of the TV programs

Programs 2 and 12 are considered *excellent* and *verygood*; programs 10, 11 and 9 are mostly *unknown*, and so on.

It is important to note that, in the absence of parallax, the response category *dontknow* is very influential in both methods CA and TCA, and it reveals a central important feature of the data: in TCA, on the first axis the category *dontknow* attains its maximum value of its relative contribution, $|SRC| = 500$, see equation (9).

3.2 Rodent species abundance data set

Table 2 displays an abundance data of size 28×9 , where 9 species of rodents have been counted at each of 28 sites in California. For the interested reader, we identify the 9 rodents by their scientific names: *rod1*=*Rt.rattus*, *rod2*=*Mus.musculus*, *rod3*=*Pm.californicus*, *rod4*=*Pm.eremicus*, *rod5*=*Rs.megalotis*, *rod6*=*N.fuscipes*, *rod7* =*N.lepida*, *rod8*=*Pg.fallax*, and *rod9*=*M.californicus*. Genus abbreviations are: *Rt* (Rattus), *Rs* (Reithrodontomys), *Mus* (Mus), *Pm* (Peromyscus), *Pg* (Perognathus), *N* (Neotoma) and *M* (Microtus). Rattus and Mus, the first 2 rodents, are invasive species, whereas the others are native. This data set was proposed in 2014 as an exercise in a course on an ecology workshop in UBC in Canada; the workshop site mentions that the data set is downloaded from the web site of Quinn and Keough (2002), and it can be found at

<https://www.zoology.ubc.ca/~bio501/R/workshops/workshops-multivariate-methods/>

It is interesting to see the 9 steps that were suggested by the instructor (we quote):

1) Download the file and read into a data frame in R. Inspect the table to get a sense of which species are abundant and which are rare, which are widely distributed and which occur infrequently.

2) Carry out a correspondence analysis using these data. Extract two axes from the species abundance data at sites. How strongly are the site and species data correlated along the two axes?

3) Plot the results from (2). Overlap of points may make it difficult to identify some plots and species (unfortunately there's no built-in "jitter" option for this plot). You can use the species scores to help identify them.

4) Use the plot in (3) and the species scores to interpret the results of your analysis. How are each of the species contributing to the correspondence axes? Do you notice any differences between the invasive and native species in their distributions?

5) As you probably surmised, the results of the first round of analysis were chiefly driven by the introduced species. To examine the native species as well, create a new data frame with *Rattus* and *Mus* deleted. This will generate some sites with no species present. Delete these sites from the new data frame.

6) Carry out a correspondence analysis on the native species. Extract two axes from the species abundance data at sites. How strongly are the species and site data correlated?

7) Plot the results from your analysis in (6). Is the plot useful in helping you to identify which species tend to co-occur? And which species tend not to occur together? Confirm this by looking at the original data. Are your interpretations correct?

8) Based on the plot in (7), which sites tend to have similar species composition? Which have different species assemblages? Confirm this by looking at the original data.

9) Based on the same plot, can you match the species to specific sites? Confirm this by looking at the original data.

We see that essentially the instructor suggests Greenacre's approach in dealing with this data set.

Figures 2 and 3 display the maps of dimensions 1-2 and 3-4 produced by CA and TCA respectively: they are completely different, so we are in the presence of a parallax. Examining the data set in Table 2, we see that it has, in particular three specificities: rare observations such as rodents 1 and 9, a zero-block structure and relatively high-valued cells. The *sparsity index* $= 166/252 = 65.87\%$. Looking at the dispersion values in Table 2, it seems that in CA there are four principal dimensions to interpret, and three in TCA.

Our main result is the following: *The two diagrams in Figure 2, which represent the best two-dimensional maps obtained by CA and TCA, jointly summarize the information content of the data set.* This result is based on the the interpretation of Figures 2 and 3, that we present some details.

3.2.1 Correspondence analysis

First, we state what facets of the data characterize the CA solution, then provide further details.

The highlighted subset of sites, 7-11, 14-17, 21-22, 24-25, which are completely associated only with the invasive rodents 1 and 2, characterizes the CA solution. Further, note that the weight of this subset of sites is $82/1002 = 8.18\%$, which is quite small. This is a well known phenomenon in multiple correspondence analysis, see for instance Choulakian, Allard and Simonetti (2013).

Let us interpret the CA biplot, the upper diagram in Figure 2. In Table 2, we note that $RC_1(rod2) = 750$; so the first axis in the CA map is dominated by rodent 2; the second axis is dominated by rodent 1, because $RC_2(rod1) = 854$. Rodents 1 and 2 are invasive: so the first CA dimension in Figure 2 separates the invasive species from the native species, which is a very important discriminatory concept in ecology. And, the second CA dimension in Figure 2 separates rodent 1 from rodent 2 within the invasive species. The two invasive species and their associated sites are fenced by segments in the CA map of Figure 2 and in the TCA map of Figure 3, which shows that these two diagrams admit the same interpretation.

3.2.2 Taxicab correspondence analysis

Let us interpret the TCA biplot, the lower diagram in Figure 2. We note that the two invasive species are grouped and found in the first quadrant of the TCA map; further, they are associated with the 13 highlighted subset

of sites that we enumerated above. The SRC_1 and SRC_2 of the rodents, displayed in Table 2, show that the TCA map is dominated by the 4 most frequent species: rodents 2, 6, 3 and 4; and each of them occupy a quadrant in the TCA map.

Let us interpret the most frequent ($freq$) species rodent 3 ($freq = 467$ out of 1002): it dominates the third quadrant, and it is associated with site3 ($freq = 36$), site5 ($freq = 63$), site13 ($freq = 39$), site18 ($freq = 78$), site27 ($freq = 29$) and site28 ($freq = 10$). Rod3 is also associated with rod5, their positions are quite near on Figure 2; looking at the entries in the column of rod5, we see that its high frequency sites are site27 ($freq = 10$), site18 ($freq = 10$), site6 ($freq = 12$), site5 ($freq = 11$); further these high frequency sites 27, 18, 6 and 5 also characterize rod3. We also note that site6 is associated with both species rod3 ($freq = 48$) and rod4 ($freq = 35$), and its position is in between rod3 and rod4; however it is found in quadrant 3, because $(35/125) > 48/467$.

3.2.3 Comparison

In the presence of a parallax, by comparing the first two principal dimensions in CA and TCA, we note the following two facts:

a) Rodent 2, with nonnegligeable weight (around 10%), has a very high influence on the first principal axis in CA ($RC_1(rod2) = 750$); but it distributes its influence onto the first two principal axes in TCA ($SRC_1(rod2) = -196$ and $SRC_2(rod2) = -238$).

b) Rodent 1 is a rare influential point in CA ($weight = 1.4\%$ and $RC_2(rod1) = 854$); but is no more influential in TCA ($SRC_1(rod1) = -23$ and $SRC_2(rod1) = -26$).

We conclude that in Figure 2, the CA map emphasized some particular aspects of the data set; while the TCA map revealed the central abundances in Table 2.

3.3 The Colors of Music data set

The *Colors of Music* data in Table 3 is a contingency table of size 10×9 taken from Abdi and Bera (2014), where 9 denotes the number of music categories and 10 the number of color categories. Abdi and Bera collected data from 22 participants, where each participant after listening to a piece of music associated it to a particular color. The pieces of music were:

- 1) the music of a video game (*Video*)

- 2) a Jazz song (*Jazz*)
- 3) a country and western song (*Country*)
- 4) a rap song (*Rap*)
- 5) a pop song (*Pop*)
- 6) an extract of the opera Carmen (*Opera*)
- 7) the low F note played on a piano (*LowF*)
- 8) the middle F note played on the same piano (*MiddleF*)
- 9) the high F note still played on the same piano (*HighF*).

Following Abdi and Bera, we interpret only the first two principal dimensions. Figure 4 displays the maps produced by CA and TCA, respectively: We note that the dispositions of the points on the two maps are quite different, so we are in the presence of a parallax. We note that the *sparsity index* = $19/90 = 21.11\%$.

The first axis of the CA map is dominated by the *black* color, $RC_1(\text{black}) = 726$ in Table 4, which is associated with *Rap* and *LowF* categories of music; the second axis is dominated by the *brown* color, $RC_1(\text{brown}) = 545$ in Table 4, which is associated with *MiddleF* and *Pop* music. In the second quadrant of the CA map, we find a medley of categories of colors (*purple*, *red*, *pink*, *orange* and *white*) and music (*HighF*, *Video*, *Opera* and *Jazz*). Note that the fourth quadrant is almost empty. Essentially, the CA map emphasizes the 4 highlighted cells in Table 3.

We interpret the four quadrants of the TCA map separately. The first quadrant shows the association of the *Rap* and *LowF* categories with the *black* color. The second quadrant shows the association of *Opera* and *HighF* with the *white* color: Note that the relative frequency of *Opera* given *White* is $4/14$ and the relative frequency of *HighF* given *White* is $5/14$. The third quadrant associates the group of (*Jazz*, *country* and *Video*) with (*purple*, *orange* and *yellow*) globally; but looking into the contingency table we can see more details, such as: *Jazz* is associated with (*orange*, *yellow*, *blue*); *country* music is associated with (*yellow*, *green*); and *Video* music with (*yellow*, *purple*). The fourth quadrant shows the association of *MiddleF* and *Pop* music with (*brown*, *green*, *blue*). This interpretation can be concisely summarized as: the first principal axis opposes dark colors to the bright colors. The second axis shows oppositions within the subgroups: within the dark colors black opposes to brown; within the bright colors white opposes to yellow and blue.

Finally, it is up to the researcher to use his judgement in the choice between the CA map or TCA map in Figure 4.

4 Conclusion

The fundamental aim of CA and TCA is to produce interpretable maps that reflect central contents in a data set. The parallax phenomenon positively associated with sparse contingency tables, shows that sometimes CA maps emphasize a particular feature of data; that is, a map produced by CA or TCA is dependent on the underlying geometry, Euclidean or Taxicab. Based on our experience, we suggest the analysis of a data set by both methods CA and TCA: Like a cubist painting where an object is painted from different angles, sometimes the views are similar (no parallax), and at other times not similar (there is a parallax). In particular for sparse contingency tables, in case there is a parallax, the comparison may reveal: either, CA and TCA complement and enrich each other as shown in the analysis of the second data set; or, the researcher uses his subjective knowledge to choose between the two methods, as shown by the analysis of the third data set.

References

- Abdi, H. and Bera, M. (2014). Correspondence analysis. In Alhajj, R. and Rokne, J. (eds.), "*Encyclopedia of Social Networks and Mining*", pp. 274-284. NY: Springer Verlag.
- Beh, E. and Lombardo, R. (2014). *Correspondence Analysis: Theory, Practice and New Strategies*. N.Y: Wiley.
- Benzécri, J.P. (1976). Sur le codage réduit d'un vecteur de description en analyse des correspondances. *Les Cahiers de l'analyse des données*, 1(2), 127-136.
- Benzécri, J.P. (1973). *L'Analyse des Données: Vol. 2: L'Analyse des Correspondances*. Paris: Dunod.
- Benzécri, J.P (1992). *Correspondence Analysis Handbook*. N.Y: Marcel Dekker.
- Choulakian, V. (2006). Taxicab correspondence analysis. *Psychometrika*, 71, 333-345
- Choulakian, V. (2008). Taxicab correspondence analysis of contingency tables with one heavyweight column. *Psychometrika*, 73, 309-319.
- Choulakian, V., Kasparian, S., Miyake, M., Akama, H., Makoshi, N., Nakagawa, M. (2006). A statistical analysis of synoptic gospels. *JADT'2006*, pp. 281-288.
- Choulakian, V., Allard, J. and Simonetti, B. (2013). Multiple taxicab correspondence analysis of a survey related to health services. *Journal of*

Data Science, 11(2), 205-229.

Choulakian, V., Simonetti, B. and Gia, T.P. (2014). Some further aspects of taxicab correspondence analysis. *Statistical Methods and Applications*, available online.

Gifi, A. (1990). *Nonlinear Multivariate Analysis*. N.Y: Wiley.

Greenacre, M. (1984). *Theory and Applications of Correspondence Analysis*. Academic Press, London.

Greenacre, M. (2013). The contributions of rare objects in correspondence analysis. *Ecology*, 94(1), 241-249.

Le Roux, B. and Rouanet, H. (2004). *Geometric Data Analysis. From Correspondence Analysis to Structured Data Analysis*. Dordrecht: Kluwer-Springer.

Murtagh, F. (2005). *Correspondence Analysis and Data Coding with Java and R*. Boca Raton, FL., Chapman & Hall/CRC.

Nishisato, S. (1984). Forced classification: A simple application of a quantification method. *Psychometrika*, 49(1), 25-36.

Nishisato, S. (2007). *Mutidimensional nonlinear descriptive analysis*. Chapman & Hall/CRC, Boca Raton.

Nishisato, S. (1998). Graphing is believing: interpretable graphs for dual scaling. In Blasius, J. and Greenacre, M. (eds.), " *Visualization of Categorical Data*", Academic Press, NY, 185-196.

Nowak, E. and Bar-Hen, A. (2005). Influence function and correspondence analysis. *Journal of Statistical Planning and Inference*, 134, 26-35.

Pisier, G. (2012). Grothendieck's theorem, past and present. *Bulletin of the American Mathematical Society*, 49 (2), 237-323.

Quinn, G. and Keough, M. (2002). *Experimental Design and Data Analysis for Biologists*. Cambridge Univ. Press, Cambridge, UK.

Rao, C.R. (1995). A review of canonical coordinates and an alternative to correspondence analysis. *Qüestiió*, 19, 23-63.

Schlick, Th. (2000). *Readings in the philosophy of Science: from positivism to post modernism*. Mayfield Publishing Company, Mountain View, California.

Table 1: TV progams data.

programs	excellent	verygood	good	average	bad	noopinion	dontknow
1	9	28	89	124	51	19	71
2	31	87	165	63	24	4	17
3	7	21	65	103	83	8	103
4	3	26	121	142	45	11	43
5	17	40	117	111	83	16	7
6	8	35	115	119	78	6	28
7	4	22	73	56	77	12	147
8	15	44	102	83	32	25	90
9	5	18	63	61	15	9	219
10	8	15	40	37	8	12	271
11	5	16	64	54	15	17	220
12	29	87	140	62	24	9	40
13	12	18	89	95	41	9	127
total	153	457	1243	1110	576	157	1383
RC_1	24	83	106	45	40	1	700
RC_2	128	285	63	181	330	2	11
SRC_1	-28	-96	-165	-137	-73	-2	500
SRC_2	-82	-235	-173	222	278	-10	0

Table 2: Rodent species abundance data.

<i>Sites</i>	rod1	rod2	rod3	rod4	rod5	rod6	rod7	rod8	rod9
1		13	3	1	1	2			
2		1	57	65	9	16	8	2	3
3		4	36		2	9			
4		4	53	1	5	30		18	3
5		2	63	21	11	16			
6		1	48	35	12	8	12	2	2
7		11							
8		16							
9	3	8							
10	1	2							
11		9							
12		3	1		5	16		7	
13		4	39		4	12			
14	1	3							
15		11							
16		4							
17	3								
18		2	78		10	14		4	
19			1						
20	3		27	1					
21	2	1							
22		3							
23					2	8		2	
24	1								
25		5							
26			22			11		2	
27			29		10	9		1	
28			10	1		1			
total	<i>14</i>	107	467	125	71	152	20	38	8
λ_{α}^{TCA}	0.478	0.422	0.347	0.138	0.120	0.091	0.061	0.010	
λ_{α}^{CA}	0.864	0.678	0.536	0.391	0.189	0.157	0.107	0.045	
RC_1	127	750	59	29	9	15	5	4	2
RC_2	854	140	3	0	0	2	0	1	0
SRC_1	-23	-196	298	-221	22	135	-51	44	-8
SRC_2	-26	-238	202	224	32	-139	42	-95	-1

Table 3: Colors of Music data.

<i>Colors</i>	video	jazz	country	rap	pop	opera	lowF	highF	middleF
red	4	2	4	4	1	2	2	4	1
orange	3	4	2	2	1	1		3	2
yellow	6	4	5	2	3	1	1	3	
green	2		5	1	3	3	3	1	5
blue	2	5		1	4	1	2	1	3
purple	3	3	1			3		2	1
white					1	4	1	5	3
black		2		11	1	3	10	1	1
pink	2	1	1		2	4		2	
brown		1	4	1	6		3		6
total	22	22	22	22	22	22	22	22	22
λ_{α}^{TCA}	0.406	0.358	0.325	0.20	0.125	0.107	0.045	0.023	
λ_{α}^{CA}	0.537	0.440	0.372	0.269	0.184	0.131	0.055	0.013	

Table 4: Colors of Music data: CA and TCA relative contributions.

<i>Colors</i>	RC_1	RC_2	SRC_1	SRC_2	<i>Music</i>	RC_1	RC_2	SRC_1	SRC_2
<i>red</i>	1	56	-66	42	<i>Video</i>	113	86	-155	-53
<i>orange</i>	31	25	-75	-52	<i>Jazz</i>	25	44	-55	-98
<i>yellow</i>	53	27	-127	-108	<i>Country</i>	33	55	-30	-102
<i>green</i>	1	144	44	-65	<i>Rap</i>	379	91	94	160
<i>blue</i>	2	21	39	-100	<i>Pop</i>	6	234	94	-122
<i>purple</i>	87	77	-119	-14	<i>Opera</i>	22	61	-80	132
<i>white</i>	26	2	-30	108	<i>LowF</i>	350	4	193	88
<i>black</i>	726	75	251	326	<i>HighF</i>	70	95	-180	120
<i>pink</i>	68	28	-83	24	<i>MiddleF</i>	2	330	119	-125
<i>brown</i>	5	545	166	-161					
total	1000	1000	1000	1000	total	1000	1000	1000	1000

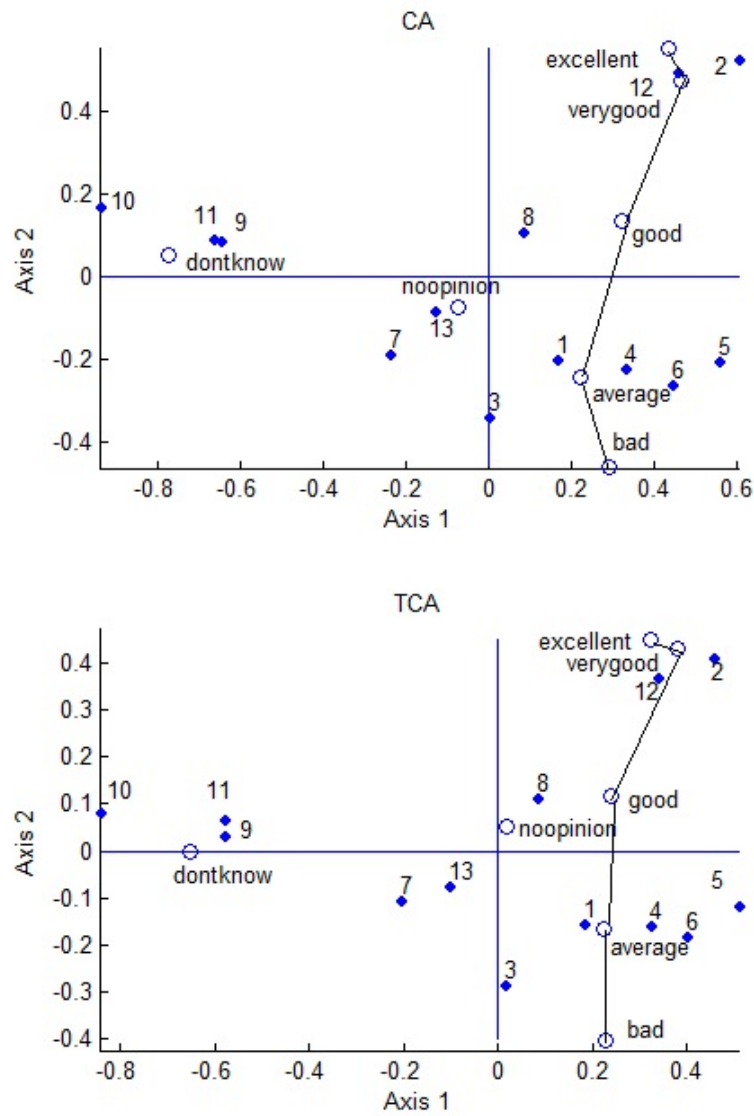


Figure 1: CA and TCA biplots of TV Programs data.

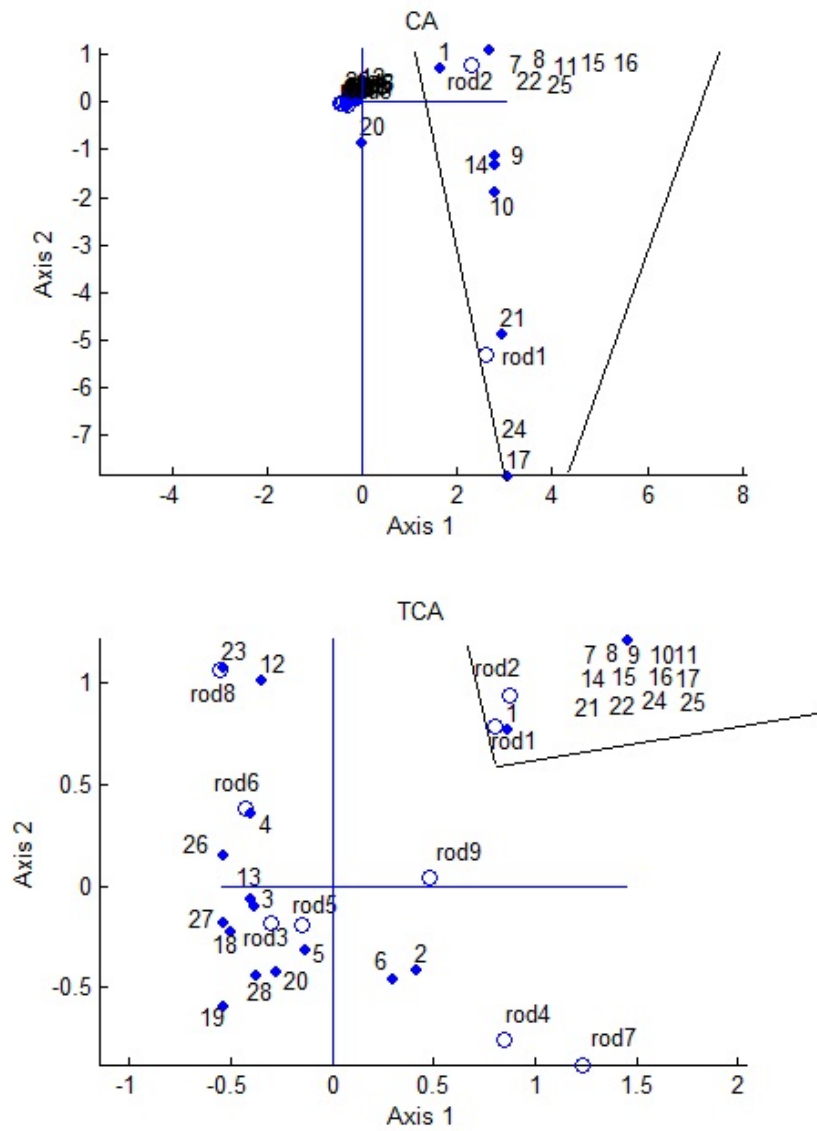


Figure 2: CA and TCA biplots of Rodents data.

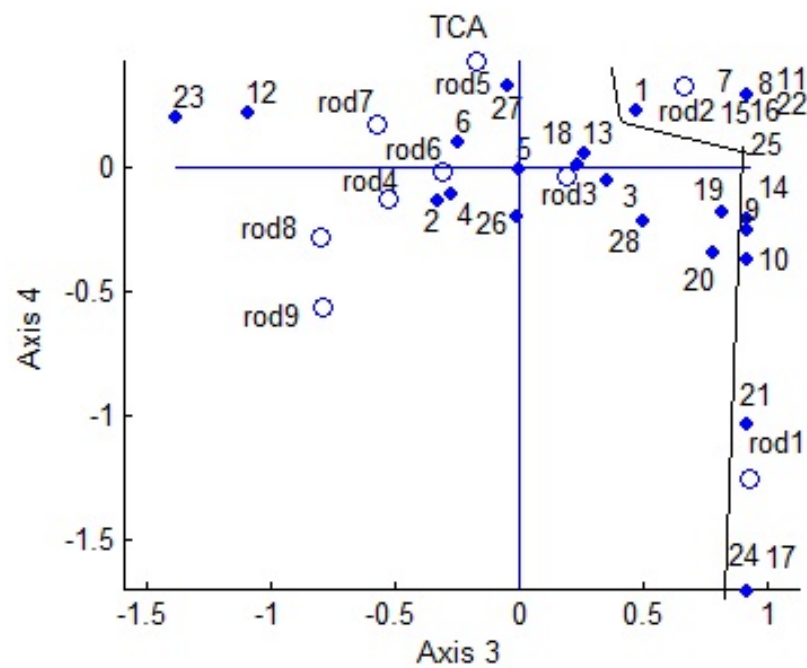
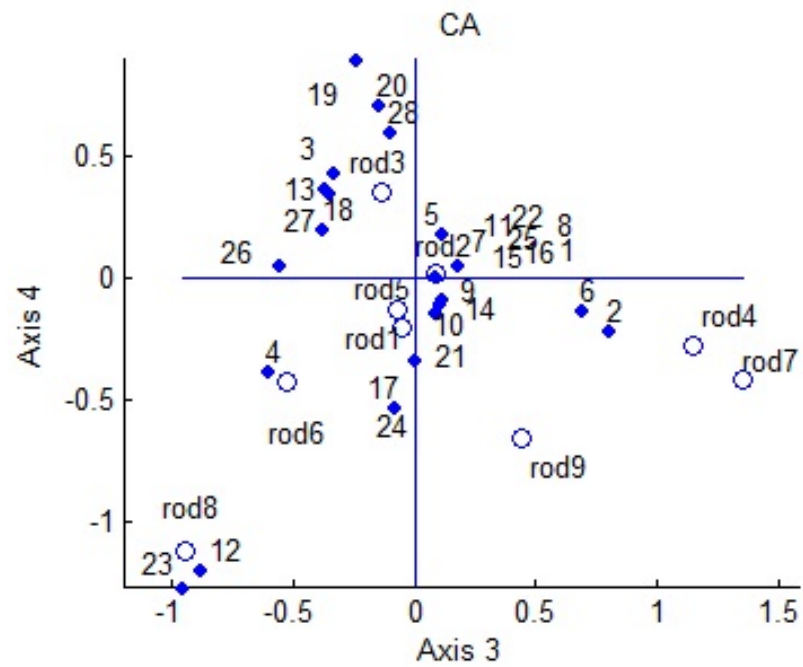


Figure 3: CA and TCA biplots of Rodents data.

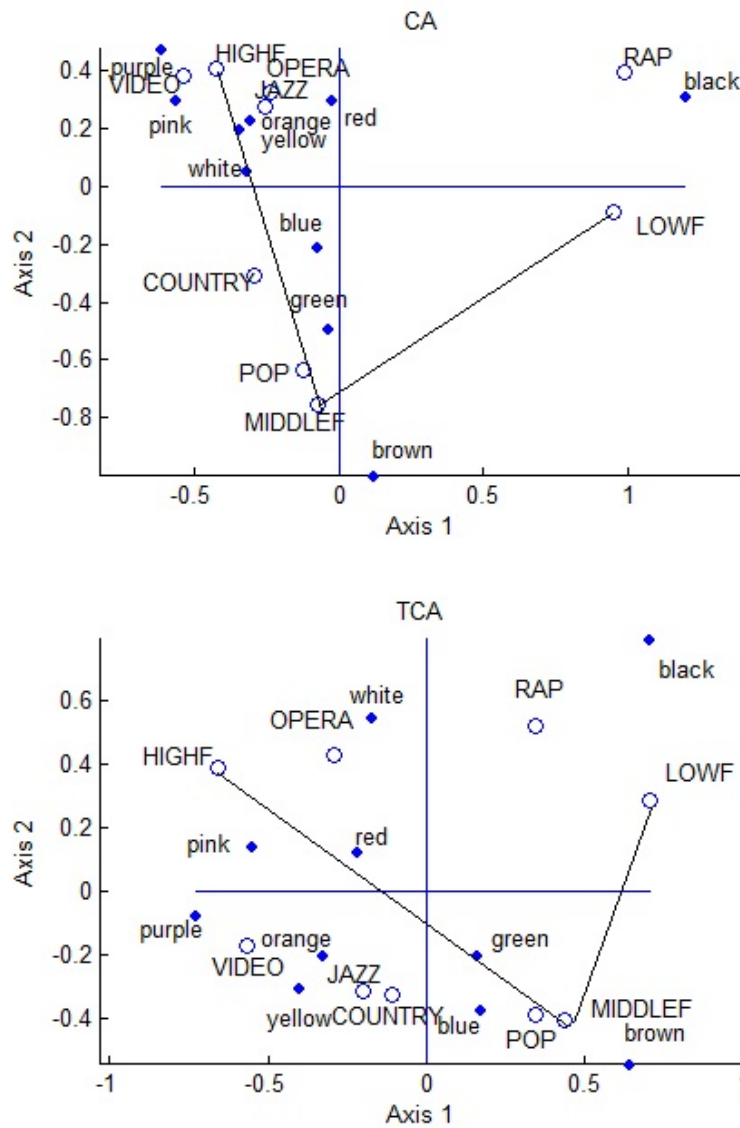


Figure 4: CA and TCA biplots of Colors of Music data.